Unstable periodic orbits and the symbolic dynamics of the complex Hénon map

Ofer Biham and Wolfgang Wenzel
Department of Physics, Ohio State University, Columbus, Ohio 43210
(Received 20 February 1990)

A numerical technique for the calculation of unstable periodic orbits of chaotic maps in the complex plane is presented. Applying this technique to the complex Hénon map we show that it can find *all* the 2^p real and complex periodic orbits of any given order p. The real periodic orbits coincide with those obtained by a similar algorithm for the ordinary Hénon map that we have proposed earlier, and thus verify its completeness. The method provides a new definition of symbolic dynamics for the Hénon map, which holds for both the real and complex periodic orbits. It provides a computational framework that applies to all limits of this map on a common footing, unlike the conventional techniques in which one needs different algorithms for calculations involving strange attractors, strange repellers, and various types of Julia sets.

I. INTRODUCTION

Chaotic behavior in low-dimensional dynamical systems has been studied extensively in recent years in the context of real maps (such as the Hénon map),[1] and also in the context of complex one-dimensional maps.[2–6] Real maps exhibit strange attractors and repellers in phase space, while the complex maps give rise to fractal sets called Julia sets. These structures can be characterized by their scaling properties such as Liapunov exponents, fractal dimensions and topological entropies.

It is widely accepted that a most useful way to study the chaotic dynamics and to characterize the underlying fractal sets is by considering the set of unstable periodic orbits embedded in them.[7–15] It was shown that scaling properties of these sets, such as the Hausdorff dimension and the spectrum of singularities $f(\alpha)$ (Ref. 16) can be directly related to properties of the unstable periodic orbits such as their Liapunov exponents. However, until recently no useful technique for the calculation of unstable periodic orbits in dynamical systems had been available. Map iteration techniques can be applied only to short unstable cycles since chaotic attractors exhibit sensitivity to initial conditions and numerical errors grow exponentially with the length of the cycle.[17] In the case of a strange repeller[18] the situation is even worse since for almost all initial conditions the trajectory tends to escape to infinity.

In a recent paper we have presented a different numerical technique that allows us to calculate unstable periodic orbits of arbitrary length to any desired accuracy for a certain class of maps.[19] Our method is based on the observation that the dynamics of maps such as the Hénon map, although dissipative, can be derived from a Hamiltonian. This Hamiltonian is constructed in such a way that its spatial degrees of freedom are equivalent to the temporal degrees of freedom of the map. In particular, there is a one-to-one correspondence between trajectories of the map and extremum static configurations of the Hamiltonian. This equivalence applies in both the regular and chaotic regimes. Therefore, by calculating the extremal configurations of the corresponding Hamiltonian, we could find unstable periodic orbits of the map to any desired accuracy even in the chaotic regime. We applied the method to the Hénon map, which is a two-dimensional quadratic map of the form[20]

$$\begin{aligned} x_{n+1} &= a - x_n^2 + b u_n \ , \\ u_{n+1} &= x_n \ . \end{aligned} \tag{1.1}$$

For this map we performed a systematic calculation of unstable periodic orbits and used the results to calculate the topological entropy and fractal dimension.

Here we briefly describe the general procedure of calculating the unstable periodic orbits of a given map. The calculation is done in a few steps: (a) We first find the Hamiltonian $H(\{x_n\})$ (for which the Euler-Lagrange equation is equivalent to the map). The static extrema of this Hamiltonian are in a one-to-one correspondence with the trajectories of the map. (b) We examine the symmetries of this Hamiltonian and find how many extrema it may have (since we are interested in periodic orbits we count only extrema which have the appropriate boundary conditions). Then we try to identify these extrema by giving them symbolic names, such that each of these extremum configurations $x_1, \ldots, x_p$ will be identified by a sequence $S_1, \ldots, S_p$, where S_i are integers. This symbolic representation depends on the particular map and there is no general way to find it. For the Hénon map, $S_i = \pm 1$.[19] (c) We choose random initial conditions x_n, $n = 1, \ldots, p$, and impose a periodic boundary condition $x_{p+1} = x_1$. (d) In order to find the extremum configuration (and thus the periodic orbit) associated with a given symbol sequence S_n, $n = 1, \ldots, p$, we introduce an artificial dynamics that converges to this particular extremum. The symbols S_n appear as parameters in this dynamics. The dynamical equations take the general form

$$\frac{dx_n}{dt} = -S_n F_n, \quad n = 1, \ldots, p \ , \tag{1.2}$$

where t is an artificial time and F_n is the force which is derived from the corresponding Hamiltonian. The symbols $S_n = \pm 1$ play an important role in choosing the direction in which this dynamics flows and thus determine which extremum it will converge to. We previously applied these ideas to real maps such as the Hénon map[19] and the dissipative standard map.[21]

In this paper we generalize the method to chaotic maps in the complex plane and apply it to a complex version of the Hénon map. Using Bezout's theorem[22] we find that the Hénon map has 2^p isolated periodic orbits of order p (including cyclic permutations, repetitions of shorter periodic orbits, and degeneracies). For generic values of the parameters our method finds all the 2^p periodic orbits of a given order p, and in particular all the real ones. These real periodic orbits coincide with the ones obtained from the algorithm that we proposed for the real Hénon map.[19] This provides a strong argument of completeness that could not be derived from the real algorithm, namely that no periodic orbits are missed.

Our numerical tests show that the symbol sequences S_n, $n=1,\ldots,p$, identify the periodic orbits uniquely and can be used as an alternative definition of symbolic dynamics of periodic orbits. This symbolic dynamics applies for both real and complex orbits. Moreover, it allows us to follow any particular periodic orbit associated with a given symbol sequence, while the parameters of the map are varied continuously.

The paper is organized as follows. In Sec. II we describe the algorithm for finding periodic orbits of the complex Hénon map. Our numerical results are presented in Sec. III and the symbolic dynamics is considered in Sec. IV. In Sec. V we summarize our results.

II. METHOD

We consider a complex version of the Hénon map which takes the following form:

$$\begin{aligned} z_{n+1} &= A - z_n^2 + B w_n \ , \\ w_{n+1} &= z_n \ , \end{aligned} \tag{2.1}$$

where z_n and w_n are complex variables given by $z_n = x_n + i y_n$ and $w_n = u_n + i v_n$, and the parameters $A = a + i\alpha$ and $B = b + i\beta$ can have a nonzero imaginary part.

When A and B are real, this map coincides with the ordinary Hénon map, provided that the initial conditions for the variables z and w are real. In particular, the $b=1$ case corresponds to the Hamiltonian Hénon map. For $0 \le b < 1$ the map is dissipative, while for $b=0$ it becomes the logistic map, which is one dimensional. The real Hénon map exhibits a rich variety of dynamic behavior with stable fixed points or periodic cycles in some regions of parameter space and chaotic motion on a strange attractor in other regions. It also exhibits strange repellers, from which the trajectories tend to be repelled. These trajectories either escape to infinity or converge to a stable periodic orbit that may coexist with the strange repeller. The real Hénon map has been studied extensively in recent years.[23–26] Another case that has been previously studied is the $b=0$ limit of the complex map. In this case the map exhibits fractal objects called Julia sets. There are a few different types of Julia sets. In some cases the Julia set is the boundary between two basins of attraction while in other cases it is the set of points that do not escape to infinity under iteration of the map. There are a few methods for the calculation of these objects, but not one of them is general enough to apply in all cases.

In the following we present our algorithm for the calculation of unstable (and stable) periodic orbits in the complex Hénon map. This algorithm applies in all limits of the map and therefore allows us to treat all cases such as strange attractors, strange repellers, and all types of Julia sets on a common footing. In this analysis we will eliminate the variable w_n from the map and obtain

$$z_{n+1} = A - z_n^2 + B z_{n-1} \ . \tag{2.2}$$

By decomposing the map (2.2) into real and imaginary parts we find

$$x_{n+1} = a - x_n^2 + y_n^2 + b x_{n-1} - \beta y_{n-1} \ , \tag{2.3}$$

$$y_{n+1} = \alpha - 2 x_n y_n + b y_{n-1} + \beta x_{n-1} \ . \tag{2.4}$$

This is a four-dimensional map since each step depends on the two previous values of both the real and imaginary parts.

We will now describe the method and calculate the periodic orbits of the complex Hénon map. We will first construct a Hamiltonian in such a way that its spatial behavior will be equivalent to the temporal behavior of the map. In particular, we will require a one-to-one correspondence between trajectories of the map and extremum static configurations of the Hamiltonian. Then we will introduce an artificial dynamics which converges to any particular extremum identified by a sequence $S_1,\ldots,S_p$ where $S_n = \pm 1$ and p is the length of the corresponding periodic orbit.

In the case that the parameter B is real (namely $\beta=0$), we can construct a real Hamiltonian H_R for which there is a one-to-one correspondence between its extremum configurations and the trajectories of the map (when B is complex, H_R, which still takes the same form, turns out to be complex). This Hamiltonian takes the following form:

$$H_R = \sum_n (-B)^{-n} \Big[x_n (x_{n+1} - x_{n-1}) - y_n (y_{n+1} - y_{n-1}) - \left[\frac{1}{B} + 1 \right] (a x_n - \tfrac{1}{3} x_n^3 + x_n y_n^2 - \alpha y_n) \Big] . \tag{2.5}$$

It can be interpreted as describing an infinite chain of atoms in a two-dimensional potential. Here (x_n, y_n) is the position of the nth atom in the x-y plane. Since we are interested only in static extremum configurations, in this paper we neglect the kinetic energy associated with (2.5) and consider only the potential energy.

The potential energy (2.5) contains two terms: the first one describes the interactions among the atoms while the

second term describes their interaction with the underlying potential. Note that the nth atom interacts only with the $(n-1)$th and $(n+1)$th atoms, which are not necessarily its nearest neighbors in the two-dimensional configuration space. In this Hamiltonian the ordinary cyclic permutation symmetry $x_n \to x_{n+1}$, $y_n \to y_{n+1}$ is replaced by a lower symmetry which is a combination of a cyclic permutation and a rescaling transformation of the form $x_n \to x_{n+1}$, $y_n \to y_{n+1}$, $H \to (-B)^{-1}H$. This property reflects the dissipative nature of the corresponding map. The potential (2.5) is not bounded from below and therefore this model does not have a ground state but only metastable states.

The force that applies on the nth atom has two components

$$F_{nx} = -\partial H_R / \partial x_n \tag{2.6}$$

and

$$F_{ny} = -\partial H_R / \partial y_n \ , \tag{2.7}$$

where

$$\partial H_R / \partial x_n = -(-B)^{-n} \left[\frac{1}{B} + 1 \right] \times (-x_{n+1} + a - x_n^2 + y_n^2 + B x_{n-1}) \tag{2.8}$$

and

$$\partial H_R / \partial y_n = (-B)^{-n} \left[\frac{1}{B} + 1 \right] \times (-y_{n+1} + \alpha - 2 x_n y_n + B y_{n-1}) \ . \tag{2.9}$$

When the chain is in a stable or unstable equilibrium $F_{nx} = F_{ny} = 0$. In this case the equation $F_{nx} = 0$ is equivalent to the real part of the map (2.3) while $F_{ny} = 0$ is equivalent to the imaginary part (2.4). We thus conclude that there is a one-to-one correspondence between the trajectories of the complex Hénon map (2.1) and extremum static configurations of the Hamiltonian (2.5). According to the general framework presented in Ref. 19, one should now introduce an appropriate artificial dynamics which will converge to the extrema of this Hamiltonian. However, it turns out that such a dynamics is unstable and does not converge to the desired extrema. This is due to the fact that the present system is more complicated and has more degrees of freedom. We find that the complex Hénon map can be derived from two different Hamiltonians and they both should be combined in order to obtain a convergent dynamics.

The second Hamiltonian H_I is constructed such that $F_{nx} = 0$ is equivalent to the imaginary part of the map (2.4) while $F_{ny} = 0$ is equivalent to the real part (2.3). This Hamiltonian takes the form

$$H_I = \sum_n (-B)^{-n} [x_n (y_{n+1} - y_{n-1}) + y_n (x_{n+1} - x_{n-1}) - \left[\frac{1}{B} + 1 \right] (a y_n + \tfrac{1}{3} y_n^3 - x_n^2 y_n + \alpha x_n)] \ . \tag{2.10}$$

Since these two Hamiltonians correspond to the same map they must have the same set of extrema.

Our aim now is to find a systematic scheme which will allow us to calculate any particular extremum of these Hamiltonians. In particular we concentrate on the calculation of extrema associated with periodic orbits. This calculation is done as follows. We first construct a family of symbol sequences such that any symbol sequence corresponds to one particular orbit. This construction depends on the problem at hand and there is no general way to find it. For the Hénon map one needs two symbols such that each periodic orbit of order p corresponds to a sequence $S_1, \ldots, S_p$, where $S_n = \pm 1$. We then introduce an artificial dynamics that converges to the extremum associated with that particular sequence. This artificial dynamics is based on a combination of the forces generated by the two Hamiltonians described before. We find that the Hamiltonians H_R and H_I can be combined to a complex Hamiltonian $H = H_R + i H_I$ from which the desired artificial dynamics can be derived. This complex Hamiltonian, associated with the map (2.1), takes the form

$$H = \sum_n (-B)^{-n} [z_n (z_{n+1} - z_{n-1}) - \left[\frac{1}{B} + 1 \right] (A z_n - \tfrac{1}{3} z_n^3)] \ . \tag{2.11}$$

Note that when the parameter B is real (namely $\beta = 0$), H_R and H_I are the real and imaginary parts of H, while for $\beta \neq 0$ they also become complex. However, our method, which will now be formulated on the basis of (2.11), applies even for complex B.

In this complex formulation the force which applies on the nth atom in the chain is given by $F_n = -\partial H / \partial z_n$, which takes the form

$$F_n = (-B)^{-n} \left[\frac{1}{B} + 1 \right] (-z_{n+1} + A - z_n^2 + B z_{n-1}) \ . \tag{2.12}$$

When the chain is in a stable or unstable equilibrium [namely an extremum static configuration of (2.11)], $F_n = 0$ for all n. One can easily see that this set of equations is equivalent to the map, and therefore there is a one-to-one correspondence between trajectories of the map (2.1) and extremum configurations of the complex Hamiltonian (2.11). In the following we will use the complex Hamiltonian to calculate unstable periodic orbits of the Hénon map.

In our calculation we identify each periodic orbit z_n, $n = 1, \ldots, p$ by a symbolic name S_n, $n = 1, \ldots, p$, where $S_n = \pm 1$. One can construct 2^p such symbol sequences which correspond to the 2^p real and complex periodic orbits of order p. Consider a particular periodic orbit of order p, associated with a given symbol sequence $S_1, \ldots, S_p$. To calculate this particular orbit we introduce an artificial dynamics defined by

$$\frac{dz_n}{dt} = C_n F_n, \quad n = 1, \ldots, p \tag{2.13}$$

where

$$C_n=(-1)^n[S_n-i\,\mathrm{sgn}(y_n)] \tag{2.14}$$

and F_n is given by (2.12). If B is real, our dynamics can be written in terms of the real variables[27]

$$\frac{dx_n}{dt}=(-1)^{n+1}\left[S_n\frac{\partial H_R}{\partial x_n}+\mathrm{sgn}(y_n)\frac{\partial H_I}{\partial x_n}\right],$$
$$\frac{dy_n}{dt}=(-1)^{n}\left[Sn\frac{\partial H_R}{\partial y_n}+\mathrm{sgn}(y_n)\frac{\partial H_I}{\partial y_n}\right]. \tag{2.15}$$

Since we are interested only in the resulting fixed point to which this dynamics converges, where $F_n=0$, it is allowed to neglect the prefactor $(B)^{-n}(1+1/B)$ on the right-hand side of (2.12) and (2.15). This involves no approximation, and no information is lost. As a result the set of dynamic equations exhibits a cyclic permutation symmetry which is not a symmetry of the Hamiltonian. This higher symmetry is important in order to obtain fast convergence, since otherwise the atoms on one side of the chain evolve very fast while the ones on the other side are very slow. In case that B is complex it is necessary to eliminate this prefactor since it is complex and mixes the real and imaginary parts of the force.

We then obtain the following equations:

$$\frac{dx_n}{dt}=S_n(-x_{n+1}+a-x_n^2+y_n^2+bx_{n-1}-\beta y_{n-1})$$
$$+\mathrm{sgn}(y_n)\left[-y_{n+1}+\alpha-2x_ny_n+\beta x_{n-1}+by_{n-1}\right] \tag{2.16}$$

and

$$\frac{dy_n}{dt}=S_n\left[-y_{n+1}+\alpha-2x_ny_n+\beta x_{n-1}+by_{n-1}\right]$$
$$-\mathrm{sgn}(y_n)\left[-x_{n+1}+a-x_n^2+y_n^2+bx_{n-1}-\beta y_{n-1}\right]. \tag{2.17}$$

In practice we solve Eqs. (2.16) and (2.17) until all forces become smaller than a test value ($|F_n|<\epsilon$ where typically $\epsilon<10^{-9}$). Since only the final configuration is of interest we can use a fourth-order Runge-Kutta method with a relatively large step size (typically $h=0.1$). A similar technique was previously applied to the study of critical behavior in the Frenkel-Kontorova model.[28] The initial condition is chosen such that $|z_n|$, $n=1,\ldots,p$, are all small with respect to $\sqrt{|A|}$. Periodic boundary conditions are then imposed by taking $z_{p+1}=z_1$. This dynamics converges to a fixed point such that $z_1,\ldots,z_p$ is the extremum of H (and thus the periodic orbit) specified by the given symbol sequence. This allows us to perform a systematic calculation of all the periodic orbits of a given order p. In some rare cases the dynamics converges to a limit cycle rather than a fixed point. In order to obtain convergence in these cases one needs some numerical tricks discussed in Sec. III.

III. RESULTS AND DISCUSSION

To test our procedure we have computed all the real and complex periodic orbits up to order $p=16$ and selected periodic orbits up to order 1000 for $A=1.4$, $B=0.3$. The method allows us to eliminate the calculation of cyclic permutations as well as orbits which are repetitions of lower-order cycles, leading to savings in computation time of at least a factor p.

Using this method we find all the 2^p periodic orbits of order p and in particular all the real orbits, which coincide with the ones obtained from the real algorithm. This provides a strong argument for the completeness of the method, namely that no orbits are missed.

Each periodic orbit of order p corresponds to a root of $F_n=0$, $n=1,\ldots,p$, where F_n is given by (2.12). This is a system of p coupled quadratic polynomials, and therefore, according to Bezout's theorem,[22] has at most 2^p isolated roots in the entire complex plane, which add up to exactly 2^p if the multiplicity of roots is taken into account. As a result we find that there are 2^p real and complex periodic orbits of order p.

The method provides a natural way to identify periodic orbits using the sequences $S_1,\ldots,S_p$. Since our method finds all the periodic orbits, and each one of them has a unique symbol sequence, we suggest that this sequence can be used as an alternative definition of symbolic dynamics for the Hénon map. These aspects will be discussed in Sec. IV.

The complex periodic orbits of the Hénon map occur in a four-dimensional space defined by (z_n,z_{n-1}) or $(x_n,y_n,x_{n-1},y_{n-1})$ and therefore are hard to visualize. Here we project the set of periodic orbits on the real plane (x_n,x_{n-1}), on the imaginary plane (y_n,y_{n-1}), and on the (x_n,y_n) plane. The projections are shown in Fig. 1. for $a=1.4$ and $b=0.3$, including all periodic orbits up to order 10.

When $B=0$ the map becomes one dimensional. In this case the periodic orbits are two dimensional, in the (x_n,y_n) plane. The closure of the set of periodic orbits is called Julia set. Julia sets are typically repellers, and therefore are not easy to calculate. Two methods are ordinarily used for their calculation: the boundary scanning method and the inverse iteration method.[5] The first method is useful only for Julia sets which are on the boundary between two different basins of attraction. In this method one divides the phase space into a large number of pixels, and then identifies the pixels which are on the boundary between the two basins of attraction. In the inverse iteration method one first finds the unstable fixed point of the map and then calculates its preimages by iterating the map backwards. The preimages are dense in the Julia set. In Fig. 2 we show the periodic points up to order 10 for $A=-i$, $B=0$. The closure of this set of points is a Julia set of the dendrite type, while its complement diverges to infinity under iteration of the map.

When the parameters of the map are varied smoothly and the periodic orbits change in a continuous fashion. Typically, when the parameters A and B are real, periodic orbits become complex in pairs when the parameter a

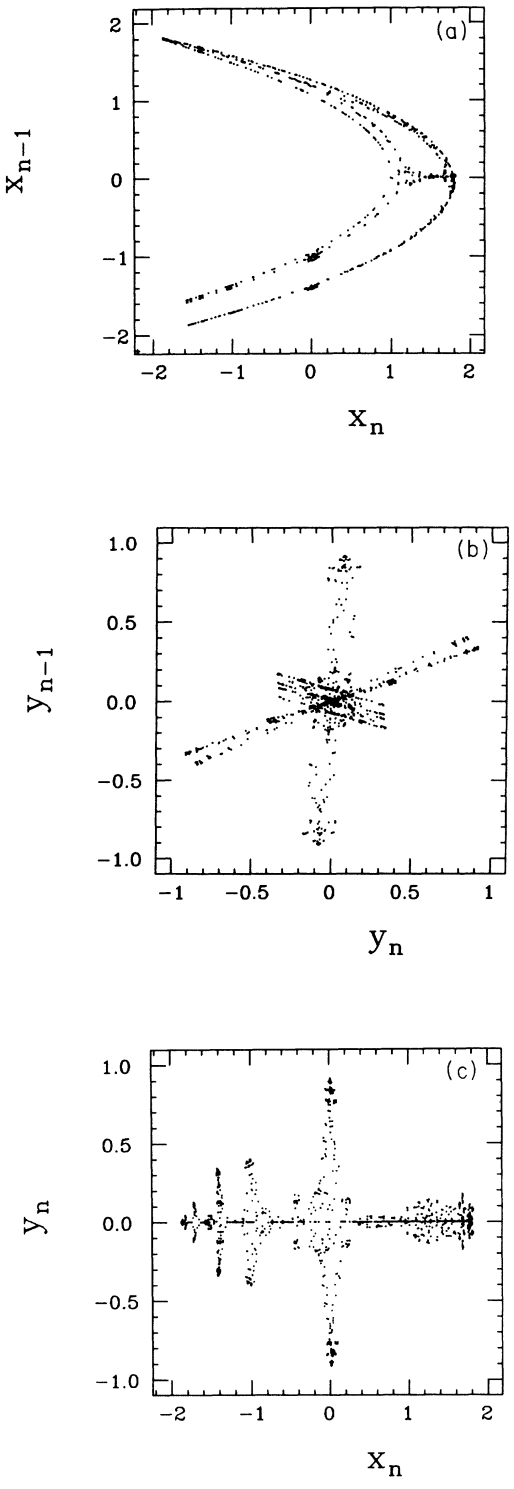

FIG. 1. Real and complex periodic points of order $p \leq 10$ for the Hénon map at $A=1.4$, $B=0.3$. Since the phase space of this map is four dimensional with the variables x_n, x_{n-1}, y_n, and y_{n-1}, we can only plot projections of it. The projection on the real plane (x_n, x_{n-1}) is shown in (a). One can recognize the general shape of the ordinary attractor, while the additional points belong to the complex periodic orbits. The projection on the imaginary plane (y_n, y_{n-1}) is shown in (b). In (c) we show the projection on the (x_n, y_n) plane. One can see that the complex orbits tend to accumulate in some regions along the x_n axis.

decreases below a critical value a_c associated with the given pair. Below a_c these pairs of orbits are complex conjugate, at a_c they are degenerate, while for $a > a_c$ they are different real orbits. There are also orbits, of even order p, which form no pairs since they consist of pairs of points which are mutually complex conjugate. The bifurcations that give rise to pairs of real periodic orbits are tangent bifurcations, while the ones in which a single orbit appears are period-doubling bifurcations.

In Fig. 3 we show the evolution of one periodic orbit of order 7, as a function of the parameter a. The coordinates x_n and y_n vary continuously as a function of a. For large a the imaginary part is zero. As a decreases, at $a=a_c$ there is a transition where the imaginary part becomes nonzero. The absolute value of the larger Liapunov number $|\lambda|$ is also shown. It decreases in the vicinity of a_c, creating a region of relative stability around this orbit. Such regions appear in nonhyperbolic systems and can affect the convergence of calculations involving scaling properties such as fractal dimensions.

In our numerical studies we found that most periodic

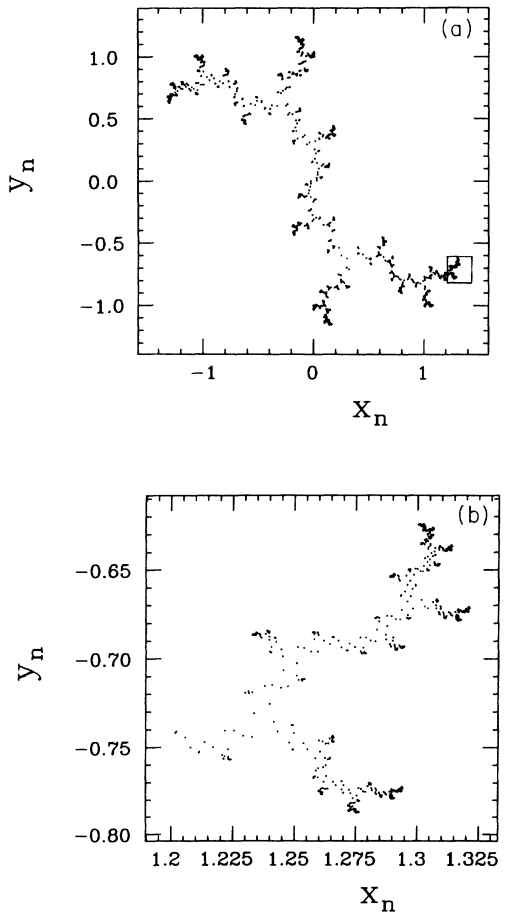

FIG. 2. (a) Periodic points order $p \leq 10$ associated with the Julia set at $A=-i$, $B=0$. The periodic orbits are dense on the Julia set. (b) Magnified view of the squared region in (a) which shows the self-similarity of this structure.

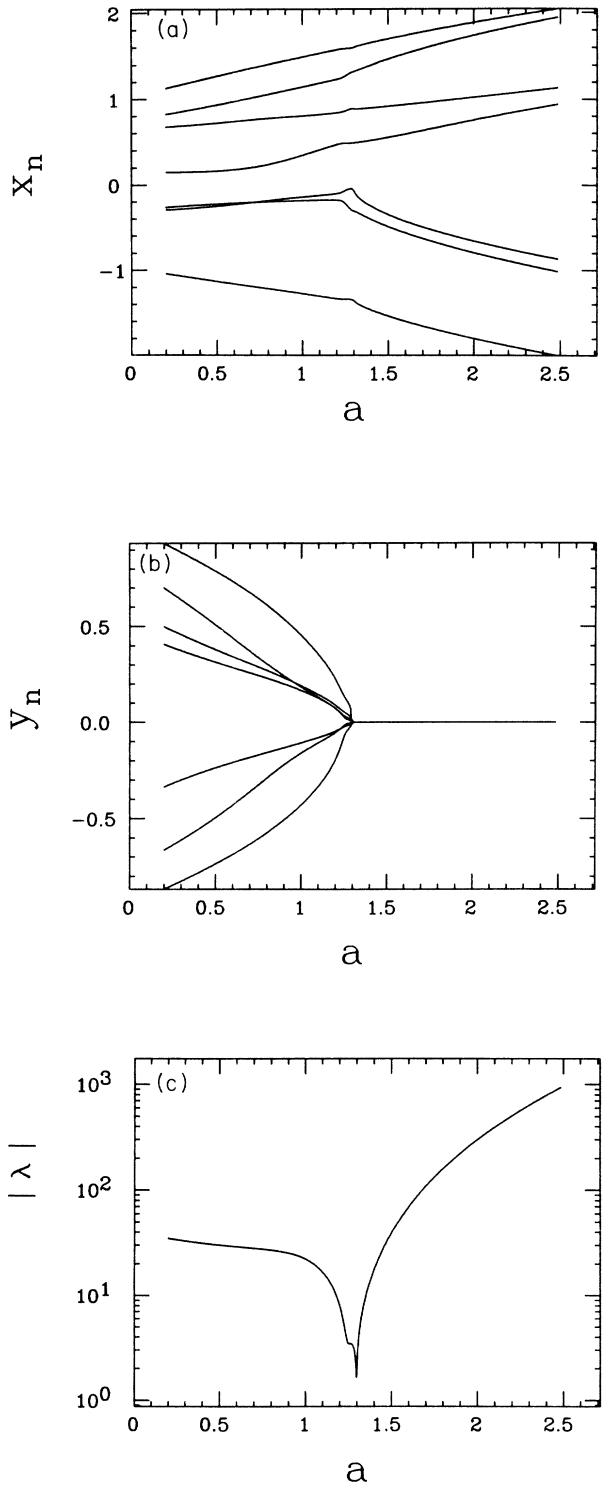

FIG. 3. Variables x_n and y_n and the absolute value of the larger Liapunov number $|\lambda|$ of the periodic orbit associated with the symbol sequence 1110100 as a function of a for $b=0.3$ ($\alpha=\beta=0$). (a) Real variables x_n which change continuously as a function of the parameter a. (b) Imaginary variables y_n are zero for $a>a_c$ when this periodic orbit is real, and become nonzero below a_c when this periodic orbit becomes complex. (c) Absolute value of the larger Liapunov number $|\lambda|$. When a decreases towards a_c, $|\lambda|$ decreases to 1, and then increases again when the orbit becomes complex.

orbits are found with no difficulty. In these calculations the method is used in a straightforward fashion with no adjustment of any parameters. However, in some rare cases the artificial dynamics does not converge to a fixed point but rather to a limit cycle. These orbits that did not converge should be treated separately. We found that these difficulties occur in the vicinity of the point where the given orbit switches from real to complex. The problem is solved by introducing a parameter which controls the relative speeds with which Eqs. (2.16) and (2.17) evolve. In practice we multiply the right-hand side of (2.17) by a constant factor Δ and change its value until convergence is obtained. As an example, we found that for $a=1.0$, $b=0.54$ our complex algorithm goes to a limit cycle when the symbol sequence 11101000 ($p=8$) is examined.[29] In this case convergence to the appropriate fixed point is obtained by taking $\Delta>1.43$, finding the period orbit associated with this symbol sequence. This orbit turns out to be real, and in agreement with the result of the real algorithm.

Another problem which may occur is that if two orbits are very close to each other, the algorithm may converge twice to the same orbit and miss the other one creating an apparent degeneracy.[30] This problem can be solved by starting the calculation at a different point in parameter space, where these orbits are far away from each other. Then the parameters are varied slowly and simultaneously with the iteration of the artificial dynamics towards the desired point in parameter space. Doing so we follow each one of these orbits from a point where they are well separated and the degeneracy is removed. This trick is also useful in order to remove a trivial degeneracy which may occur when the parameters A and B are real. In this case most complex periodic orbits appear in pairs or orbits which are complex conjugate of each other. However, the dynamical equations (2.16) and (2.17) are invariant under $y_n \rightarrow -y_n$ and therefore cannot distinguish between the two complex-conjugate orbits. Using this trick with initial $\alpha \neq 0$ removes this possible degeneracy.

Similar problems may occur in the calculation of periodic orbits in the real Hénon map.[31] The problem there is solved using numerical tricks which are similar to the ones described here. Another useful trick is to allow different time steps for different equations. These modifications do not affect the validity of the results since we are interested only in the convergent solution after all the forces decrease to zero.

IV. SYMBOLIC DYNAMICS OF THE HÉNON MAP

Symbolic dynamics is a useful tool for the understanding of the topology of the attractor, and is an important step in any attempt to apply formalisms of statistical mechanics to the study of chaos. In this framework one tries to identify each periodic orbit x_n, $n=1,\ldots,p$, by a unique symbolic name S_n, $n=1,\ldots,p$, where for the Hénon map S_n can take two symbolic values such as 0 and 1. This is usually done dividing the phase space into

two or more regions and giving each one of them a symbolic name. It was observed that for the ordinary Hénon attractor (1.4,0.3), the line $x=0$ provides an approximate partition by choosing $S_n=1$ for $x_n>0$ and $S_n=0$ for $x_n<0$. However, this is not a good partition since in some cases two orbits may correspond to the same symbol sequence.

In order to obtain a unique symbolic dynamics Grassberger and Kantz[32] suggested a different partition. Their partition is constructed by first calculating a set of points of homoclinic tangencies, then choosing a subset of them as primary tangencies and connecting them with a line. This line provides a good partition in the sense that each periodic orbit has a unique symbol sequence.

A good partition can also be obtained by taking the $x=0$ line as a starting point and then examining the symbolic dynamics hierarchically for periodic orbits of increasing order.[33] When two different orbits are found to have the same symbolic dynamics the partition line is shifted locally such that the point which has the smallest $|x_n|$ in one of the two orbits moves to the other side such that the degeneracy is removed.

One can gain insight concerning the symbolic dynamics by considering the topology of the Hénon attractor, which behaves like a pruned horseshoe map. Numerically it was found that in the topological pruning space there is a line which divides it into two parts; one associated with the allowed symbol sequences and the other part with the disallowed ones.[13,34] This line is called pruning front.

In all these approaches one should first calculate a large number of periodic orbits, and then start organizing them according to some rule. In case of the Hénon map one needs a single partition which will divide the phase space into two parts. The partition should be refined step by step for periodic orbits of increasing order. This calculation becomes more complicated and less reliable for high orders.

In our method the symbolic dynamics is an integral part of the method and does not need any extra computation since we first choose a symbol sequence and only then calculate the periodic orbit associated with this particular sequence. We obtained numerical evidence that the method applies in all regions of parameter space that have been studied and a unique symbol sequence was found for both real and complex periodic orbits. Note that for the complex orbits the partition is a three-dimensional manifold in a four-dimensional phase space and thus hard to construct and to visualize.

By varying the parameters of the map we can follow any particular orbit over all the parameter space. We find that as the parameters are varied the structure of the periodic orbit $\{z_n\}$ changes continuously, while its identity is kept via the symbol sequence $\{S_n\}$. We used these ideas to examine the relation between unstable periodic orbits on the attractor at $a=1.4$, $b=0.3$ and their counterparts at $a=1.0$, $b=0.54$. We found that by varying the parameters between these two points, following a particular periodic orbit, the variables $\{z_n\}$ change continuously and the procedure is reversible. Therefore we conclude that any symbol sequence that we examined corresponds to the same periodic orbit for both values of the parameters.

This result is interesting in light of the observation made in Ref. 31 that our symbolic dynamics is identical to the one of Grassberger and Kantz[32] for $a=1.4$, $b=0.3$ but not for $a=1.0$, $b=0.54$. It may indicate that in their procedure, in which they find the primary tangencies numerically and then connect them by lines to form a partition, the symbol sequences associated with two different periodic orbits may switch as the parameters a and b are varied.

V. CONCLUSION

We have presented a numerical technique for the calculation of unstable periodic orbits in complex maps. For the complex Hénon map we found, using Bezout's theorem, that there are 2^p real and complex periodic orbits of order p. Applying our method to this map we have shown that in generic cases it can find all the 2^p periodic orbits of order p. In the calculation we identify each periodic orbit $z_1,\ldots,z_p$ by a symbol sequence $S_1,\ldots,S_p$ where $S_n=\pm 1$. Since we find that these symbol sequences uniquely identify the periodic orbits, we propose that they can be used as an alternative definition of symbolic dynamics. Our method allows us to follow any particular periodic orbit while varying the parameters of the map. We find that when the parameters vary smoothly, the structure of each periodic orbit changes continuously, while its symbol sequence remains unchanged.

We have shown that in typical cases our method applies automatically with no need to adjust any parameters or any other human intervention. In some cases, however, which we identified to occur around the point where a real periodic orbit becomes complex, one needs to adjust a parameter in order to obtain convergence, otherwise the method converges to a limit cycle.

Further study is needed in order to obtain a theoretical understanding of the method. The artificial dynamics that we use can be cast into the framework of coupled differential equations. Such systems, in general, can exhibit not only fixed points but also limit cycles and strange attractors. The success of our method results from the fact that in typical cases the artificial dynamics converges to a fixed point. It will be interesting to study the method within the framework of coupled differential equations in order to obtain a better understanding of its properties.

ACKNOWLEDGMENTS

We thank C. Jayaprakash and M. Kvale for many helpful discussions. This work was supported in part by the National Science Foundation Grant No. DMR8451911, and by IBM (for W.W.), by the Department of Energy, and by the Ohio Supercomputer Center, which provided us with CRAY time.

[1]See, e.g., *Chaos,* edited by Hao Bai-Lin (World Scientific, Singapore, 1984); or *Universality in Chaos,* edited by P. Cvitanovi'c (Hilger, Bristol, 1984).
[2]M. Widom, D. Bensimon, L. P. Kadanoff, and S. J. Shenker, J. Stat. Phys. **32**, 443 (1983).
[3]B. B. Mandelbrot, Physica D **7**, 224 (1983).
[4]M. H. Jensen, L. P. Kadanoff, and I. Procaccia, Phys. Rev. A **36**, 1409 (1987).
[5]D. Saupe, Physica D **28**, 358 (1987).
[6]M. Barnsley, *Fractals Everywhere* (Academic, New York, 1988).
[7]D. Auerbach, P. Cvitanovi'c, J. P. Ekmann, G. H. Gunaratne, and I. Procaccia, Phys. Rev. Lett. **58**, 2387 (1987).
[8]C. Grebogi, E. Ott, and J. A. Yorke, Phys. Rev. A **36**, 3522 (1987).
[9]S. M. Hammel, J. A. Yorke, and C. Grebogi, Complexity **3**, 136 (1987).
[10]G. H. Gunaratne and I. Procaccia, Phys. Rev. Lett. **59**, 1377 (1987).
[11]C. Grebogi, E. Ott, and J. A. Yorke, Phys. Rev. A **37**, 1711 (1988).
[12]D. Auerbach, B. O'Shaughnessy, and I. Procaccia, Phys. Rev. A **37**, 2234 (1988).
[13]P. Cvitanovi'c, G. H. Gunaratne, and I. Procaccia, Phys. Rev. A **38**, 1503 (1988).
[14]G. H. Gunaratne, M. H. Jensen, and I. Procaccia, Nonlinearity **1**, 157 (1988).
[15]P. Cvitanovi'c, Phys. Rev. Lett. **61**, 2729 (1988).
[16]T. C. Halsey, M. H. Jensen, L. P. Kadanoff, I. Procaccia, and B. I. Shraiman, Phys. Rev. A **33**, 1141 (1986).
[17]Suppose that the computer precision is $\delta = 10^{-k}$. Since the errors after n iterations increase exponentially like λ^n where $\lambda > 1$, any roundoff error expands to order unity after $n = \log_\lambda(1/\delta)$ iterations. This sets an upper bound on the length of unstable periodic cycles which can be calculated.
[18]C. Grebogi, E. Ott, and J. A. Yorke, Physica D **7**, 181 (1983).
[19]O. Biham and W. Wenzel, Phys. Rev. Lett. **63**, 819 (1989).
[20]M. Hénon, Commun. Math. Phys. **50**, 69 (1976).
[21]W. Wenzel, O. Biham, and C. Jayaprakash (unpublished).
[22]See, e.g., B. L. van der Waerden, *Modern Algebra* (Ungar, New York, 1940); W. Vogel, *Results on Bezout's Theorem* (Springer-Verlag, Berlin, 1984).
[23]S. D. Feit, Commun. Math. Phys. **61**, 249 (1978).
[24]C. Simó, J. Stat. Phys. **21**, 465 (1979).
[25]J. H. Curry, Commun. Math. Phys. **68**, 129 (1979).
[26]J. H. Curry, J. Stat. Phys. **26**, 683 (1981).
[27]Here we use the Cauchy-Rieman condition: $\partial H_R/\partial x_n = \partial H_I/\partial y_n$ and $\partial H_R/\partial y_n = -\partial H_I/\partial x_n$.
[28]M. Peyrard and S. Aubry, J. Phys. C **16**, 1593 (1983).
[29]Here, for clarity, we replace $S_n = -1$ by $S_n = 0$ while $S_n = 1$ remains unchanged.
[30]Multiple roots or closely spaced roots produce a most serious difficulty for root finding algorithms. See, e.g., *Numerical Recipes, the Art of Scientific Computing,* edited by W. H. Press, B. P. Flannery, S. A. Teukolsky, and W. T. Vetterling (Cambridge University Press, New York 1986). This book also contains an interesting discussion on the advantage of multidimensional minimization versus multidimensional root finding techniques, which is relevant to the method used here.
[31]P. Grassberger, H. Kantz, and U. Moenig, J. Phys. A **22**, 5217 (1989).
[32]P. Grassberger, and H. Kantz, Phys Lett. **113A**, 235 (1985).
[33]D. Auerbach (private communication).
[34]P. Cvitanovi'c (private communication).